Distributed estimation of vector fields*

Ana Portêlo[1], Jorge S. Marques[2], Catarina Barata[2], and João M. Lemos[1]

[1] INESC-ID, Instituto Superior Técnico, Universidade de Lisboa, Portugal,
[2] Institute for Systems and Robotics, Instituto Superior Técnico, Universidade de Lisboa, Portugal

Abstract. In many surveillance applications the area of interest is either wide or includes alleys or corners. Thus, the images from multiple cameras need to be combined and this fact motivates the use of distributed optimization approaches. This work proposes three distributed estimation approaches to motion field estimation from target trajectory data: (1) purely decentralized, without communication, (2) distributed estimation based on a cooperative game, and (3) distributed Alternating Direction Method of Multipliers (ADMM). Their performance in estimating different classes of motion fields is important to select the best approach for each application. Experiments using synthetic and real data show that (a) the cooperative game approach is very susceptible to changes in motion direction, and (b) the distributed ADMM approach is the most robust and reliable approach to estimate changing direction motion fields.

Keywords: Distributed optimization, Vector field estimation, Multi-camera, Surveillance

1 Introduction

The estimation of motion fields based on target (*e.g.*, pedestrians or vehicles) trajectories provides information about the usual motion flow of targets in a scene [1]. This information can be used in surveillance systems to detect unusual trajectories [2], plan accessibility conditions in cities [3], or for crowd analysis [4].

In many surveillance applications the area of interest is very large or includes alleys or corners. Thus, images from a single camera may not cover the entire area of interest, and the images of two or more cameras need to be combined. In this case, it is reasonable to assume that there is some overlap among the images of the different cameras to make sure the whole area is covered. Multi-camera systems involve several coherence constraints, which motivates the use of distributed optimization algorithms. While previous studies focused on target tracking using image features [5, 6], the focus of this work is to ensure coherence among the motion fields estimated using trajectory data from several cameras.

In distributed optimization algorithms, several agents estimate a set of variables without the need for a central coordinating agent, nor widespread knowledge of every variable. Distributed algorithms usually involve two steps: the

* Work supported by FCT and FEDER under contracts PTDC/EEIPRO/0426/2014 (project SPARSIS), UID/CEC/50021/2013 and UID/EEA/50009/2013

communication step and the computation step. In the communication step, each agent shares its local information (*e.g.*, the new estimates) with its neighbours. In the computation step, each agent minimizes its local cost function using information shared by its neighbours in the prior communication step. Some popular distributed estimation approaches rely on the Alternating Direction Method of Multipliers (ADMM) [7], or on game theory [8].

This work focuses on the estimation of the motion field that describes the observed target trajectories. The proposed distributed estimation approaches are: (1) a purely decentralized approach, without communication among agents, (2) a distributed estimation approach based on a cooperative game, and (3) a distributed version of ADMM. The performance of these approaches in the estimation of different types of motion fields, using different number of trajectories, and with different overlaps among camera images is important to select the best approach for each application. Moreover, it should be relevant to set-up multicamera surveillance systems according to the geometry of the scene, and to optimize existing set-ups. In this framework, the paper contributions are the distributed estimation of motion fields using the three proposed methods and the comparison of their estimation performance considering different classes of motion fields.

This work is organized as follows. Section 2 describes the dynamic model of target trajectories, the parametric motion field representation, and the basic cost function for motion field estimation. Section 3 describes the three proposed distributed estimation approaches. Section 4 presents experiments using synthetic and real target trajectory data, followed by some conclusions in Section 5.

2 Dynamic Model and Motion Field Estimation

2.1 Dynamic Model of Target Trajectories

This work assumes that the target trajectories, $\mathbf{x} = (\mathbf{x}_1, \ldots, \mathbf{x}_L)$, on the full image plane (*i.e.*, $[0,1]^2$) are driven by the motion field, $\mathbf{T}(\mathbf{x})$, according to

$$\mathbf{x}(t) = \mathbf{x}(t-1) + \mathbf{T}(\mathbf{x}(t-1)) + \mathbf{w}(t)\,, \tag{1}$$

where $\mathbf{x} \in [0,1]^2$, $\mathbf{T} : [0,1]^2 \to \mathbb{R}^2$, and $\mathbf{w}(t) \sim \mathcal{N}(0, \sigma^2\,\mathbf{I})$ is a white random perturbation.

2.2 Motion Field Representation

The motion field is defined only at the grid nodes of an over-imposed uniform grid, $\mathcal{G} = \{\mathbf{g}_i \in [0,1]^2, i = 1, \ldots, N\}$, on the full image plane. This grid contains the open scene and the target trajectories. However, the target trajectories can be defined in any image coordinate, even if it does not correspond to a grid node ($\mathbf{x} \notin \mathcal{G}$). Therefore, it is necessary to use a bilinear interpolation to represent

the motion field that drives the trajectories on any coordinate of the full image plane. The bilinear interpolation of the motion field is given by

$$\mathbf{T}(\mathbf{x}) = \sum_{i=1}^{N} \boldsymbol{\phi}_i(\mathbf{x})\, \mathbf{t}_i \,, \tag{2}$$

which is defined in $\mathbf{x} \notin \mathcal{G}$, and where $\boldsymbol{\phi}_i(\mathbf{x})$ are the interpolation coefficients, and $\mathbf{t}_i$ the motion field velocity vectors at the grid nodes.

2.3 Motion Field Estimation

The motion field, $\mathbf{T}$, that rules a set of S collected trajectories $\mathcal{X} = \{\mathbf{x}_1, \ldots, \mathbf{x}_S\}$ on the full image plane is the minimizer of the following cost function

$$f(\mathbf{T}) = \|\mathbf{V} - \mathbf{T}\,\boldsymbol{\Phi}\|_2^2 + \alpha\, \|\Delta\mathbf{T}\|_2^2 + \beta\, \|\mathbf{T}\|_1 \,, \tag{3}$$

where $\|.\|_p$, $p \in \{1, 2\}$ defines the pth norm of a vector. $\mathbf{T} \in \mathbb{R}^{2\times N}$, $\mathbf{V} \in \mathbb{R}^{2\times S\,(L-1)}$, and $\boldsymbol{\Phi} \in \mathbb{R}^{N\times S\,(L-1)}$ are given by

$$\mathbf{T} = \begin{bmatrix} \mathbf{t}_1 \ldots \mathbf{t}_N \end{bmatrix} , \tag{4}$$

$$\mathbf{V} = \begin{bmatrix} \mathbf{v}(2) \ldots \mathbf{v}(L_1) \ldots \mathbf{v}(2) \ldots \mathbf{v}(L_S) \end{bmatrix} , \tag{5}$$

$$\boldsymbol{\Phi} = \begin{bmatrix} \boldsymbol{\phi}_1(1) \ \ldots \ \boldsymbol{\phi}_1(L_1-1) \ \ldots \ \boldsymbol{\phi}_1(1) \ \ldots \ \boldsymbol{\phi}_1(L_S-1) \\ \vdots \qquad\qquad \vdots \qquad\qquad \vdots \qquad\qquad \vdots \\ \boldsymbol{\phi}_N(1) \ldots \boldsymbol{\phi}_N(L_1-1) \ldots \boldsymbol{\phi}_N(1) \ldots \boldsymbol{\phi}_N(L_S-1) \end{bmatrix} , \tag{6}$$

where matrices $\mathbf{V}$ and $\boldsymbol{\Phi}$ respectively consider the velocity, $\mathbf{v}(t) = \mathbf{x}(t) - \mathbf{x}(t-1)$, and the interpolation coefficients per grid node, for each trajectory time point. In (3), the first term is the usual data fidelity criterion, the second term refers to smoothness between pairs of neighbour grid nodes, $(\mathbf{x}_{g1},\, \mathbf{x}_{g2}) \in \mathcal{G}$, such that the velocity difference, $\Delta\mathbf{T} = \mathbf{T}(\mathbf{x}_{g1}) - \mathbf{T}(\mathbf{x}_{g2})$, should be small, and the third term refers to sparsity of the motion field.

3 Distributed Estimation Approaches

In this work, the full image plane, *i.e.*, $[0, 1]^2$, is composed of several sub-regions, $\mathcal{R} = \{1, 2, \ldots, R\}$, delimited by the fields of view of the different cameras. Each camera and the respective field of view corresponds to an estimator agent.

There is a set of estimator agents $\mathcal{A} = \{1, 2, \ldots, A\}$. An agent $i \in \mathcal{A}$ has at least one neighbour, $j \in \mathcal{N}_i$. Each agent is composed of sub-regions, $r \in \mathcal{R}_i \subset \mathcal{R}$, that may overlap with neighbour agents. An overlapping sub-region of agent j with its neighbours i is defined as $o \in \mathcal{O}_i^{(j)}$, $j \in \mathcal{N}_i$, where $\mathcal{O}_i^{(j)}$ is the set of overlapping sub-regions of agent j with its neighbours i.

Each estimator agent yields its own motion field estimate. A motion field estimate is the set of estimated velocity vectors sitting on the grid nodes that

belong to the set of sub-regions of the respective agent, *i.e.*, $\bar{\mathbf{T}}^{(i)} = \{\mathbf{t}_g\}, g \in \mathcal{R}_i$, in reference to the full image coordinate system. Whenever applicable, $\bar{\mathbf{T}}^{(i)}$ are agent-specific motion field estimates, and $\mathbf{T}_r^{(i)}$, $r \in \mathcal{R}_i$ are sub-region-specific motion field estimates.

3.1 Purely Decentralized Estimation

The first approach is a purely decentralized estimation problem in which communication among agents is not allowed. This approach aims to minimize the local cost functions, f_i defined as in (3). The problem to be solved is

$$\begin{aligned} \underset{\bar{\mathbf{T}}^{(i)}}{\text{minimize}} \quad & f_i(\bar{\mathbf{T}}^{(i)}) \\ \text{subject to} \quad & \mathbf{x}^{(i)}(t) = \mathbf{x}^{(i)}(t-1) + \bar{\mathbf{T}}^{(i)}(\mathbf{x}^{(i)}(t-1)) + \mathbf{w}(t)\,, i \in \mathcal{A}\,, \end{aligned} \tag{7}$$

for each agent i, where $\mathbf{x}^{(i)}$ are the target trajectory data within region $\mathcal{R}_i$. Because there is no communication among agents, (7) can be solved in parallel.

3.2 Distributed Estimation Based on a Cooperative Game

The second approach is based on a distributed cooperative game, which aims to minimize a global cost function. There are three actions, *i.e.* strategies, that each agent can take to solve the motion field estimation problem. Either keep the previous strategy and share the last best estimate that yielded the global minimizer; cooperate and share an altruist estimate that solves its neighbours motion field estimation problems; or defect and selfishly ask its neighbours to share what it believes to be the best input for its own motion field estimation problem. Thus, in this approach, each agent estimates its motion field, $\bar{\mathbf{T}}^{(i)}$, assuming the neighbour agents share either (a) the last best estimate, $\bar{\mathbf{T}}_b^{(j)}$; (b) the altruist estimate, $\bar{\mathbf{T}}_a^{(j)}$; or (c) the selfish estimate, $\bar{\mathbf{T}}_*^{(j)}$ [9].

The cooperative game algorithm has 2 computation instances, that can be done in parallel, and 2 communication instances. Each agent computes local motion field estimates and cost function values, and shares local motion field estimates with its neighbours and local cost function values with all agents. The problem to be solved is

$$\begin{aligned} \underset{\bar{\mathbf{T}}^{(1)},\ldots,\bar{\mathbf{T}}^{(A)}}{\text{minimize}} \quad & \sum_{i=1}^{A} f_i\big(\bar{\mathbf{T}}^{(i)} | \mathbf{v}_r^{(i)}, \mathbf{T}_o^{(j)}\big) \\ \text{subject to} \quad & \mathbf{x}^{(i)}(t) = \mathbf{x}^{(i)}(t-1) + \bar{\mathbf{T}}^{(i)}(\mathbf{x}^{(i)}(t-1)) + \mathbf{w}(t),\, i \in \mathcal{A}\,, \\ & \mathbf{v}_r^{(i)}(t) = \mathbf{x}_r^{(i)}(t) - \mathbf{x}_r^{(i)}(t-1)\,, r \in \mathcal{R}_i \setminus \mathcal{O}_j^{(i)}\,, \\ & \mathbf{T}_o^{(j)} \in \{\mathbf{T}_b^{(j)}, \mathbf{T}_*^{(j)}, \mathbf{T}_a^{(j)}\},\, o \in \mathcal{O}_i^{(j)},\, j \in \mathcal{N}_i\,, \end{aligned} \tag{8}$$

where $\mathbf{x}_r^{(i)}$ and $\mathbf{v}_r^{(i)}$ are the target trajectory data and respective velocities within agent i sub-region $r \in \mathcal{R}_i \backslash \mathcal{O}_j^{(i)}$, $j \in \mathcal{N}_i$ (where $A \backslash B$ represents the set of elements

of set A that are not in set B). In iteration k, each agent i computes its selfish motion field estimate according to

$$\bar{\mathbf{T}}_*^{(i),k+1} = \arg\min_{\bar{\mathbf{T}}^{(i)}} f_i(\bar{\mathbf{T}}^{(i)}|\mathbf{v}_r^{(i)}, \mathbf{T}_b^{(j),k}), \tag{9}$$

which is computed given local data, $\mathbf{v}_r^{(i)}$, $r \in \mathcal{R}_i \setminus \mathcal{O}_j^{(i)}$, and the neighbours best motion field estimates from the previous iteration regarding the overlapping regions, $\mathbf{T}_b^{(j),k}$. Each agent i also computes the altruist motion field estimate it wishes to receive from its neighbours according to

$$\bar{\mathbf{T}}_a^{(j),k+1} = \arg\min_{\bar{\mathbf{T}}^{(j)}} f_i(\bar{\mathbf{T}}^{(j)}|\mathbf{v}_o^{(i)}, \mathbf{T}_*^{(i),k+1}), \tag{10}$$

which is computed given the data from the overlapping regions, $\mathbf{v}_o^{(i)}$, $o \in \mathcal{O}_i^{(j)}$, $j \in \mathcal{N}_i$, and its new selfish motion field estimate from its local sub-region, $\mathbf{T}_*^{(i),k+1}$.

Then, the agents share their new estimates with their neighbours. This way, each agent can compute its local cost function, defined as in (3), where $\mathbf{V}^{(i)} = \left[\mathbf{v}_r^{(i)} \left\{\mathbf{T}_o^{(j)}\right\}_{j\in\mathcal{N}_i}\right]$ considers the neighbours possible new estimates regarding the overlapping regions. The updated local cost function values are also shared. Finally, the decision about which estimate each agent should select is made considering the sums of the local cost functions over all agents, $F = \sum_{i=1}^{A} f_i\big(\bar{\mathbf{T}}^{(i)}|\mathbf{v}_r^{(i)}, \mathbf{T}_o^{(j)}\big)$, for all the possible combinations of pairs of neighbour agents estimates, $\big(\bar{\mathbf{T}}^{(i)}, \{\mathbf{T}_o^{(j)}\}_{j\in\mathcal{N}_i}\big) \in \big\{\mathbf{T}_b^{(\cdot)}, \mathbf{T}_*^{(\cdot)}, \mathbf{T}_a^{(\cdot)}\big\}^{|\mathcal{N}_i|+1}$.

3.3 Distributed Estimation Based on ADMM

The third approach is based on the Alternating Direction Method of Multipliers (ADMM) [7]. This work follows the distributed ADMM algorithm [10], adapted to the motion field estimation problem. Each agent i only knows its own cost function, f_i defined as in (3), and the shared motion field estimates from its neighbours, $\mathbf{T}_o^{(j)}$, $o \in \mathcal{O}_i^{(j)}$, $j \in \mathcal{N}_i$. The problem to be solved is

$$\begin{aligned} \underset{\bar{\mathbf{T}}^{(1)},\ldots,\bar{\mathbf{T}}^{(A)}}{\text{minimize}} \quad & \sum_{i=1}^{A} f_i(\bar{\mathbf{T}}^{(i)}) \\ \text{subject to} \quad & \mathbf{T}_o^{(i)} = \mathbf{T}_o^{(j)},\ o \in \mathcal{O}_i^{(j)},\ j \in \mathcal{N}_i, \\ & \mathbf{x}^{(i)}(t) = \mathbf{x}^{(i)}(t-1) + \bar{\mathbf{T}}^{(i)}(\mathbf{x}^{(i)}(t-1)) + \mathbf{w}(t), i \in \mathcal{A}, \end{aligned} \tag{11}$$

where $\mathbf{x}^{(i)}$ are the target trajectory data within each agent region $\mathcal{R}_i$. The constraints translate in each agent i having a copy of the motion field estimates at its overlapping regions.

The current problem formulation is not yet a distributed optimization problem. A colouring scheme similar to [10] allows the formulation of a distributed

version of ADMM by defining

$$\tilde{\mathbf{T}}^c = \begin{cases} \{\bar{\mathbf{T}}^{(i)}\}_{i\in\mathcal{A}\cap\mathcal{C}_c}, & \text{if } j \notin \mathcal{N}_i\,, (i,j)\in\mathcal{A} \\ \emptyset, & \text{if } j \in \mathcal{N}_i\,, (i,j)\in\mathcal{A} \end{cases}, \tag{12}$$

where $\tilde{\mathbf{T}}^c$ is the set of $\bar{\mathbf{T}}^{(i)}$ from the agents with colour c. This colouring scheme applied to the constraints of (11), allows their separation into C coupled constraints, such that it is rewritten as

$$\begin{aligned} \underset{\tilde{\mathbf{T}}^1,\ldots,\tilde{\mathbf{T}}^C}{\text{minimize}} \quad & \sum_{i\in\mathcal{C}_1} f_i(\bar{\mathbf{T}}^{(i)}) + \cdots + \sum_{i\in\mathcal{C}_C} f_i(\bar{\mathbf{T}}^{(i)}) \\ \text{subject to} \quad & \tilde{\mathcal{M}}^1\,\tilde{\mathbf{T}}^1 + \cdots + \tilde{\mathcal{M}}^C\,\tilde{\mathbf{T}}^C = 0\,, \\ & \mathbf{x}^{(i)}(t) = \mathbf{x}^{(i)}(t-1) + \bar{\mathbf{T}}^{(i)}(\mathbf{x}^{(i)}(t-1)) + \mathbf{w}(t)\,, i\in\mathcal{A}\,, \end{aligned} \tag{13}$$

where $\tilde{\mathcal{M}}^c$ is the diagonal concatenation of the transpose of the neighbour-overlap (*i.e.*, node-arc) incidence matrices $\mathcal{M}_1^c$, $\mathcal{M}_2^c$, …, $\mathcal{M}_O^c$, over the set of overlapping sub-regions $o \in \mathcal{O}_i^{(j)}$, for all pairs of neighbour agents. This problem can be solved using the multi-block/distributed ADMM [10], where λ_o^{ij} is the dual variable associated to $\mathbf{T}_o^{(i)} = \mathbf{T}_o^{(j)}$, $o \in \mathcal{O}_i^{(j)}$, $j \in \mathcal{N}_i$, and $\gamma = \sum_{i\in\mathcal{C}_c}\sum_{j\in\mathcal{N}_i}\lambda_o^{ij}$. The augmented Lagrangian of (13) is

$$\mathcal{L}_\rho(\tilde{\mathbf{T}}^1,\ldots,\tilde{\mathbf{T}}^c;\gamma) = \sum_{c=1}^{C}\sum_{i\in\mathcal{C}_c} f_i(\tilde{\mathbf{T}}^{(i)}) + \sum_{c=1}^{C}\gamma^\top\,\tilde{\mathcal{M}}^c\,\tilde{\mathbf{T}}^c + \frac{\rho}{2}\Big\|\sum_{c=1}^{C}\tilde{\mathcal{M}}^c\,\tilde{\mathbf{T}}^c\Big\|^2, \tag{14}$$

with penalty parameter, $\rho > 0$. The problem to be solved consists of a sequence of C sub-problems, obtained by minimizing (14) with respect to each block $\tilde{\mathbf{T}}^c$, and of updates of the dual variable γ. The resulting Distributed-ADMM (D-ADMM) algorithm updates are

$$\tilde{\mathbf{T}}^{1,\,k+1} = \underset{\tilde{\mathbf{T}}^1}{\arg\min} \sum_{i\in\mathcal{C}_1} f_i(\bar{\mathbf{T}}^{(i)}) + \gamma^{k\top}\tilde{\mathcal{M}}^1\,\tilde{\mathbf{T}}^1 + \frac{\rho}{2}\Big\|\tilde{\mathcal{M}}^1\,\tilde{\mathbf{T}}^1 + \sum_{c=2}^{C}\tilde{\mathcal{M}}^c\,\tilde{\mathbf{T}}^{c,k}\Big\|^2, \tag{15}$$

$$\vdots$$

$$\tilde{\mathbf{T}}^{C,\,k+1} = \underset{\tilde{\mathbf{T}}^C}{\arg\min} \sum_{i\in\mathcal{C}_C} f_i(\bar{\mathbf{T}}^{(i)}) + \gamma^{k\top}\tilde{\mathcal{M}}^C\,\tilde{\mathbf{T}}^C + \frac{\rho}{2}\Big\|\sum_{c=1}^{C-1}\tilde{\mathcal{M}}^c\,\tilde{\mathbf{T}}^{c,k+1} + \tilde{\mathcal{M}}^C\,\tilde{\mathbf{T}}^C\Big\|^2, \tag{16}$$

$$\gamma^{k+1} = \gamma^k + \rho\sum_{c=1}^{C}\tilde{\mathcal{M}}^c\,\tilde{\mathbf{T}}^{c,k+1}\,. \tag{17}$$

There are $(C-1)+1$ communication instances in each iteration: (a) the agents of colour c share their new estimates with neighbour agents of colour $c+1$, and (b) all neighbour agents get the new estimates and the updated Lagrange multipliers. Each update $\tilde{\mathbf{T}}^c$ can be decomposed into $|\mathcal{C}_c|$ problems that can be solved in parallel, given that agents of the same colour cannot be neighbours.

4 Experimental Results

This section presents motion field estimation experiments, on the image plane, using synthetic and real trajectory data and the three proposed estimation approaches described above. These experiments consider only 2 estimator agents.

Motion field estimation performance is assessed both regarding the magnitude and the relative angle of the estimated pairs of vectors *via* a vector field evaluation (VFE) diagram [11], which considers the vector similarity coefficient (R_v) and the vector root mean square length (RMSL) defined as,

$$R_v = \frac{1}{N}\sum_{i=1}^{N} \mathbf{A}_i^* \cdot \mathbf{B}_i^* \,, \tag{18}$$

$$\text{RMSL} = L_V^2 = \frac{1}{N}\sum_{i=1}^{N} \|\mathbf{V}_i\|_2^2 \,, \tag{19}$$

where "$\cdot$" is the inner product between two normalized vector fields $\mathbf{A}_i^*$ and $\mathbf{B}_i^*$, with $\mathbf{V}_i^* = \frac{\mathbf{V}_i}{L_V}$ given $\mathbf{V}_i = (x_{vi}, y_{vi})$, $i = 1, 2, \ldots, N$, and $\|.\|_2$ represents the l_2-norm of a vector. These metrics respectively assess the mean of the inner product of normalized vector pairs (18), and the systematic difference in the mean vector length (19). To facilitate interpretation of the results, RMSL is normalized with respect to L_V, where V is either the known generating motion field (in the synthetic case) or the full image estimated motion field (in the real case) when the focus is accuracy assessment, or the estimated motion field from agent 1 when the focus is consensus assessment. Thus, in the figures below, values closer to the black circumference represent better performance.

The values of the cost function parameters α and β on (3) were the minimizers of the motion field estimation problem considering the full image where $\rho = 0$. Then, the D-ADMM penalty parameter, ρ, was selected to yield a good trade-off between accuracy and consensus among neighbour agent estimates. The selected parameter values were $\alpha = 0.2$, $\beta = 0.2$, and $\rho = 1$. The noise variance of the synthetic data was $\sigma^2 = 10^{-4}$. Motion field estimation depended on the number of available trajectories ($S = 5, 80$), and on the width of the overlapping region ($|o| = 1, 3, 5, 7$) within an over-imposed grid of 11×11 nodes.

4.1 Synthetic Target Trajectory Data

Synthetic data consisted on target trajectories of length L generated with different types of motion fields: (a) a circular motion field (changing motion direction); (b) a V-shaped upwards motion field (composed of two upwards diagonal motion fields – to the left or to the right).

Regarding the different types of motion field, we expected the circular motion field to highlight the robustness of the D-ADMM approach in estimating motion fields with changing direction within the overlapping region, and the susceptibility of the Cooperative game to local optima. Moreover, because the V-shape upwards motion field was created to mimic the generating motion field of the

real target trajectory data, we expected it to provide ground truth results for comparison. Regarding the conditions for motion field estimation, we expected more available trajectories to improve accuracy and consensus error of the estimates. We also expected D-ADMM to be more robust to changes in the width of the overlapping region.

Circular motion field. The top row of Figure 1 shows that higher $|o|$ yields higher angle similarity between pairs of vectors for all approaches. The Cooperative game is the approach that is most affected by changes in $|o|$. The lack of consensus between neighbour agent estimates is mostly due to differences in the relative angle of the estimated vectors (see Figure 2). This effect is due to changes in the direction of the generating motion field in the overlapping region, which are not easy to extrapolate between neighbour agents. The bottom row of Figure 1 shows that the Decentralized and the D-ADMM approaches, yield more accurate estimates than the Cooperative game approach. This effect is observed in the magnitude of the estimated vectors.

Moreover, fewer available trajectories also yield less accurate estimates for the Cooperative game and the D-ADMM approaches (see Figure 2). Regions where there are no available trajectories are the most affected, as expected.

V-shaped upwards motion field. The zoom in panels of Figure 3 show that medium $|o|$ yields better matching and more accurate vector field estimates for all approaches. The D-ADMM approach is the least affected by changes in $|o|$, and the one that yields more accurate vector field estimates (see Figure 4). This experiment, with fixed $S = 50$, serves as ground truth for comparison with the real data experiment.

4.2 Real Target Trajectory Data

The video signal was acquired using a Sony HDR-CX260 video camera with a resolution of 8.9 megapixels per frame and working at a frame rate of 30 frames per second. The targets trajectories were extracted using a tracking algorithm [12]. The trajectories were then sub-sampled at a frame rate of 1 frame per second, and the association errors were corrected. There were $S = 47$ available trajectories (see bottom-right panel of Figure 4).

V-shaped upwards motion field. Figure 5 shows that medium to high $|o|$ yields better matching and more accurate vector field estimates for all approaches. The D-ADMM approach is the least affected by changes in $|o|$, regarding consensus of the estimated vector pairs, and the one that yields more accurate estimates.

In comparison with the V-shape upwards motion field estimation using synthetic data, these results yield similar trends in consensus and accuracy assessment. Regarding the consensus, the effect of $|o|$ is larger for the estimated vector length of the real data example than in the synthetic data example, especially for the Decentralized and the Cooperative game approaches. Regarding the accuracy, the effect of $|o|$ is larger for both the relative angle and vector length of

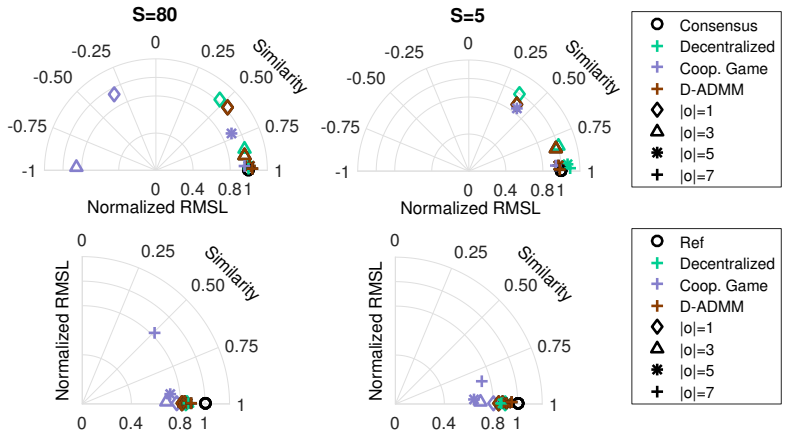

Fig. 1. Vector field diagrams to assess consensus between estimated motion fields of neighbouring agents (top row) and estimation accuracy with reference to the circular motion field (bottom row). The different colours represent each distributed estimation approach. The columns represent different available trajectories ($S = 80, 5$). The symbols represent several widths of the overlapping region ($|o| = 1, 3, 5, 7$).

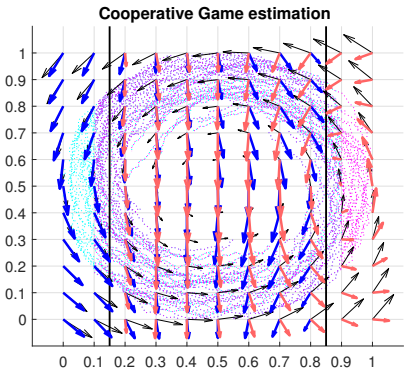

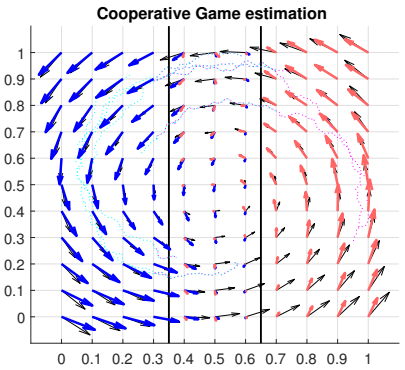

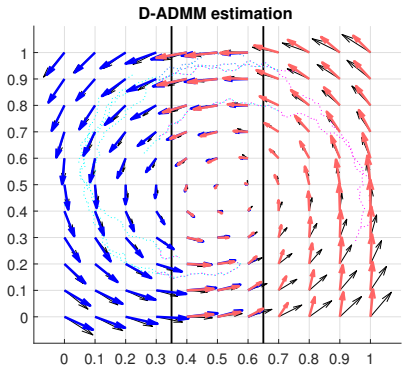

Fig. 2. Circular motion field estimation results (thick arrows). Black thin arrows are the ground truth. *Left*: motion field estimates with $S = 80$, $|o| = 7$ for the Cooperative game approach. *Below*: motion field estimates with $S = 5$, $|o| = 3$ for the Cooperative game and D-ADMM approaches. There are two estimator agents: one from the left hand side until the vertical line on the right, and the other from the vertical line on the left until the right hand side.

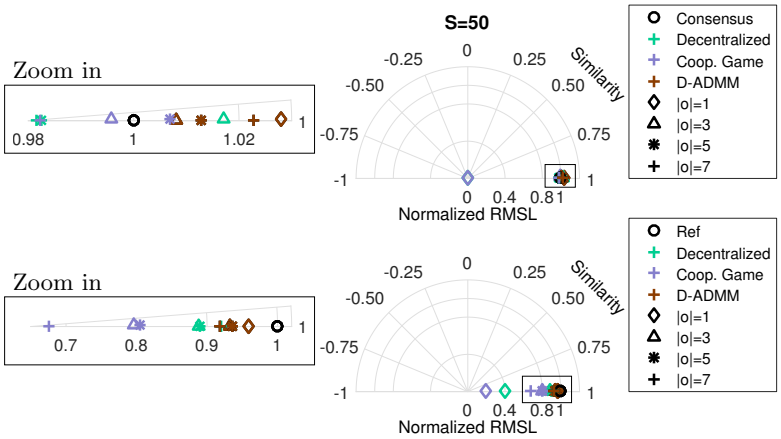

Fig. 3. Vector field diagrams to assess consensus between estimated motion fields of neighbouring agents (top row) and estimation accuracy with reference to the V-shaped upwards motion field (bottom row). The different colours represent each distributed estimation approach. The columns represent different available trajectories ($S = 80, 5$). The symbols represent several widths of the overlapping region ($|o| = 1, 3, 5, 7$).

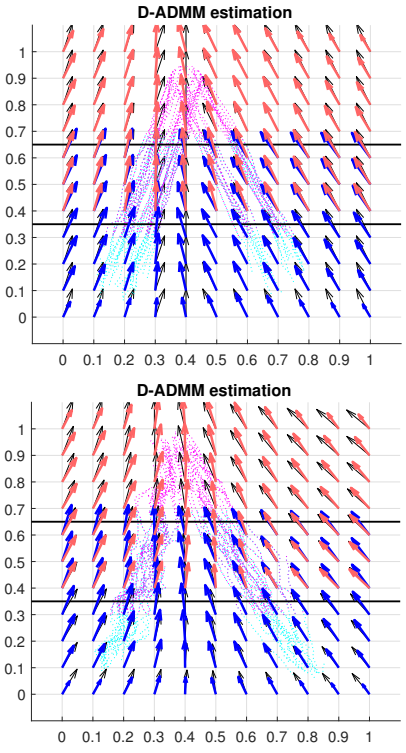

Fig. 4. V-shaped upwards motion field results (thick arrows). Black thin arrows are the ground truth. *Below*: the real data images with over-imposed trajectories. *Left*: V-shaped upwards motion field estimates for the D-ADMM approach with $|o| = 3$, using synthetic (top) and real (bottom) trajectory data. There are two estimator agents: one from the bottom until the upper horizontal line, and the other from the lower horizontal line until the top.

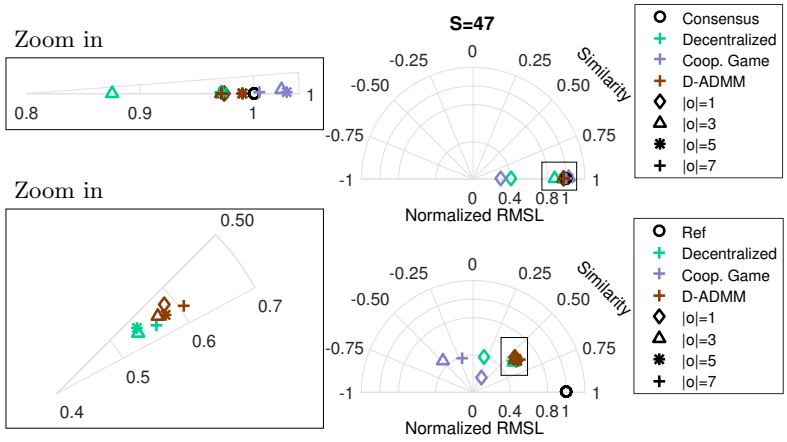

Fig. 5. Vector field diagrams to assess consensus between estimated motion fields of neighbouring agents (top row) and estimation accuracy with reference to the V-shaped upwards motion field (bottom row). The different colours represent each distributed estimation approach. The columns represent different available trajectories ($S = 80, 5$). The symbols represent several widths of the overlapping region ($|o| = 1, 3, 5, 7$).

the real data example than of the synthetic data example. This difference can be due to using low σ^2 for generating synthetic data, when compared to the real data.

5 Conclusions

This work proposes three distributed approaches to estimate motion fields from target (*e.g.*, pedestrians or vehicles) trajectories in an open scene. The motion fields are assumed to rule the target trajectories [1]. This work focuses on surveillance scenarios of very large spaces or including alleys or corners, in which cases the images from a single camera are insufficient to cover the whole area of interest. The first approach considered was a purely decentralized one without communication among estimator agents. The second approach was a distributed estimation approach based on a Cooperative game. In this scenario, the agents estimates do not necessarily converge to the optimum. The third approach was a distributed version of the ADMM algorithm. In this scenario, the goals are to obtain both accurate estimates and consensus among neighbour agents estimates.

The experiments using synthetic target trajectory data show that the D-ADMM approach is the most robust and reliable approach to estimate generating motion fields with changes in direction within the overlapping regions of neighbour agents because only the D-ADMM approach considers a flexible equality constraint among neighbour agents estimates. Contrarily, the Cooperative game

approach is very susceptible to changes in motion direction in the overlapping region of neighbour agents.

Regarding the number of available trajectories, the experiments show that fewer available trajectories hamper motion field estimation, as expected. Regarding the overlapping region, the D-ADMM approach is the most robust to different overlapping widths. Finally, the results on the V-shaped upwards motion field estimation showed that, from the proposed approaches, the D-ADMM yields more accurate and consensual estimates.

References

1. Nascimento, J.C., Figueiredo, M.A.T., Marques, J.S.: Trajectory analysis in natural images using mixtures of vector fields. In: ICIP. (2009) 4353–4356
2. Marques, J.S., Figueiredo, M.A.T.: Fast Estimation of Multiple Vector Fields: Application to Video Surveillance. In: ISPA 2011 - 7th International Symposium on Image and Signal Processing and Analysis. (2011)
3. Ferreira, N., Klosowski, J.T., Scheidegger, C.E., Silva, C.T.: Vector Field k-Means: Clustering Trajectories by Fitting Multiple Vector Fields. Eurographics Conference on Visualization (EuroVis) **32**(3) (2013)
4. Yao, H., Cavallaro, A., Bouwmans, T., Zhang, Z.: Guest Editorial Introduction to the Special Issue on Group and Crowd Behavior Analysis for Intelligent Multicamera Video Surveillance. IEEE Transaction on Circuits and Systems for Video Technology **27**(3) (2017)
5. Sankaranarayanan, A.C., Veeraraghavan, A., Chellappa, R.: Object detection, tracking and recognition for multiple smart cameras. Proceedings of the IEEE **96**(10) (2008) 1606–1624
6. Taj, M., Cavallaro, A.: Distributed and decentralized multicamera tracking. IEEE Signal Processing Magazine **28**(3) (2011)
7. Boyd, S., Parikh, N., Chu, E., Peleato, B., Eckstein, J.: Distributed Optimization and Statistical Learning via the Alternating Direction Method of Multipliers. Foundations and Trends in Machine Learning **3**(1) (2010) 1–122
8. Li, N., Marden, J.R.: Designing games for distributed optimization. IEEE Journal on Selected Topics in Signal Processing **7**(2) (2013) 230–242
9. Maestre, J.M., Muros, F.J., Fele, F., Muñoz de la Peña, D., Camacho, E.F.: Distributed MPC based on a team game. In Maestre, J.M., Negenborn, R.R., eds.: Distributed Model Predictive Control Made Easy. Springer Publishing Company, Incorporated (2013) 407–419
10. Mota, J.F., Xavier, J.M., Aguiar, P.M., Puschel, M.: Distributed Optimization with Local Domains: Applications in MPC and Network Flows. IEEE Transactions on Automatic Control **60**(7) (2015) 2004–2009
11. Xu, Z., Hou, Z., Han, Y., Guo, W.: A diagram for evaluating multiple aspects of model performance in simulating vector fields. Geoscientific Model Development **9**(12) (2016) 4365–4380
12. Veenman, C.J., Reinders, M.J.T., Backer, E.: Resolving motion correspondence for densely moving points. IEEE Trans. Pattern Anal. Mach. Intell. **23**(1) (2001) 54–72